Improved Structure and Long-life Blanket Concepts for Heliotron Reactors

A. Sagara 1), S. Imagawa 1), O. Mitarai 2), T. Dolan 1), T. Tanaka 1), Y. Kubota 1),
K. Yamazaki 1), K. Y. Watanabe 1), N. Mizuguchi 1), T. Muroga 1), N. Noda 1), O. Kaneko 1),
H. Yamada 1), N. Ohyabu 1), T. Uda 1), A. Komori 1), S. Sudo 1), and O. Motojima 1)

1) National Institute for Fusion Science, Toki, Gifu 509-5292, Japan
2) Kyushyu Tokai University, 9-1-1 Toroku, Kumamoto 862-8652, Japan

e-mail contact of main author: sagara.akio@nifs.ac.jp

Abstract. New design approaches are proposed for the LHD-type heliotron D-T demo-reactor FFHR2 to solve the key engineering issues of blanket space limitation and replacement difficulty. A major radius over 14 m is selected to permit a blanket-shield thickness of about 1 m and to reduce the neutron wall loading and toroidal field, while achieving an acceptable cost of electricity COE. Two sets of optimization are successfully carried out. One is to reduce the magnetic hoop force on the helical coil support structures by adjustment of the helical winding coil pitch parameter and the poloidal coils design, which facilitates expansion of the maintenance ports. The other is a long-life blanket concept using carbon armor tiles that soften the neutron energy spectrum incident on the self-cooled Flibe-RAF blanket. In this adaptation of the Spectral-shifter and Tritium breeder Blanket (STB) concept a local tritium breeding ratio TBR over 1.2 is feasible by optimized arrangement of the neutron multiplier Be in the carbon tiles, and the radiation shielding of the super-conducting magnet coils is also significantly improved. Using the constant cross sections of helically winding shape, the "screw coaster" concept is proposed to replace in-vessel components such as the STB armor tiles. The key R&D issues to develop the STB concept, such as radiation effects on carbon and enhanced heat transfer of Flibe, are elucidated.

1.   Introduction

Due to inherently current-less plasma, helical power reactors have attractive advantages, such as steady operation and no dangerous current disruption. Aiming at system integration for D-T fusion demo-reactors on the basis of physics and engineering results established in the LHD project [1], much progress has been made in design studies, including R&D works on engineering issues in the LHD-type heliotron power reactor FFHR [2]. In those studies the coil pitch parameter γ of continuous helical winding has been adjusted beneficially to reduce the magnetic hoop force while expanding the blanket space, and a self-cooled liquid blanket using molten salt Flibe (BeF$_2$-LiF) has been proposed, due to its advantages of low MHD pressure loss, low reactivity with air, low pressure operation, and low tritium solubility.

In the direction of decreasing reactor size, however, many issues still remain, such as insufficient tritium breeding ratio (TBR) and nuclear shielding for superconducting (SC) magnets, and replacement of blanket due to high neutron wall loading and narrowed maintenance ports due to the support structure for high field coils. Thus, if we can accept some range of increased reactor size with decreased magnetic fields, then it may be possible to overcome all these issues at the same time by improving the support structure and introducing a long–life breeder blanket. Here the first results of these new design approaches are presented.

2.   Optimized Design of a Long-life Breeder Blanket

In case of a liquid blanket, since the breeder liquid can be continuously circulated and refreshed during the reactor operation, the lifetime of blanket is essentially limited by the total displacement damage and He production in structural materials under irradiation by fusion neutrons. There are many candidates for structural materials such as reduced activation ferritic

steel (RAF), vanadium alloy, and SiC/SiC composite. In case of RAF, which has a very mature material database and is chemically compatible with Flibe, the design limit is about 15MWa/m^2 (about 120dpa). This means that the lifetime is 10 years under 1.5MW/m^2 as adopted so far in FFHR designs, and replacement is needed three times in the reactor life of 30 years. Therefore, if the effective wall loading could be reduced by a factor of 3, then no replacement would be required. This concept was proposed about 30 years ago as ISSEC (Internal Spectral Shifter and Energy Converter) by employing thick carbon shields as armor tiles on the blanket wall [3]. In this concept, therefore, the breeder blanket radioactive waste is largely reduced, while the carbon armors, low-level waste with no γ-ray, have to be replaced due to neutron damage. In that ISSEC study, however, the TBR was below 1.05 even with the Be neutron multiplier in C and 90% enriched liquid Li, and there was no practical means for actively cooling the carbon tiles below about 2000°C to avoid high carbon vapor pressure.

Figure 1 shows the new proposal of our STB (Spectral-shifter and Tritium breeder Blanket) of Flibe in the limited thickness of about 1m, where the position and thickness of the Be$_2$C layer between the 1st C and 2nd C layers and the Flibe zone are optimized as shown in Figs.2 and 3 with the MCNP-4C calculations for a simple torus model using JENDL3.2 nuclear data. Comparing with the original blanket [2] (not STB), results show that in this STB the flux of fast neutrons (> 0.1MeV) at the first
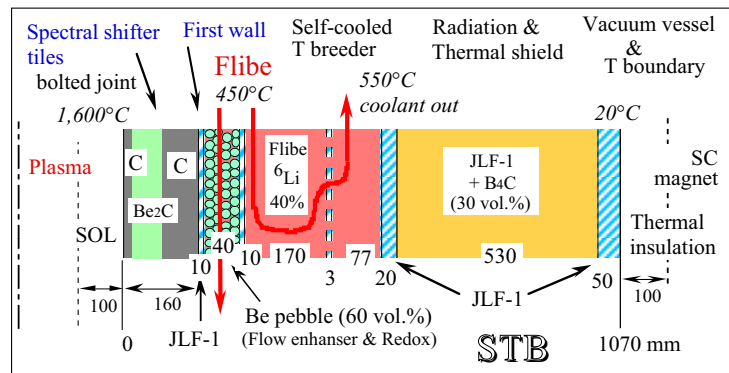

FIG.1   The radial build of the STB for FFHR2m1&2.

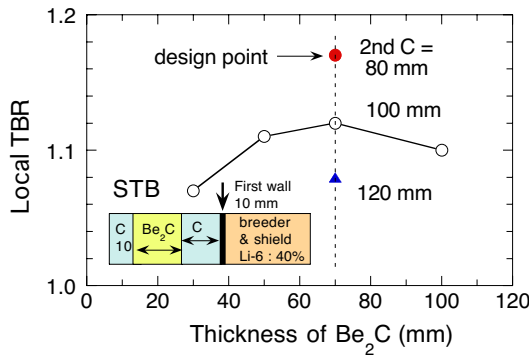FIG.2   Local TBR as a function of the thickness of Be$_2$C zone.
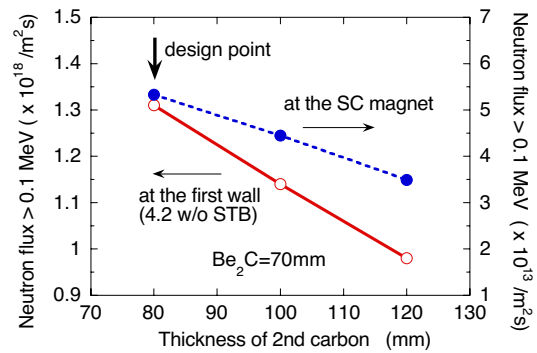

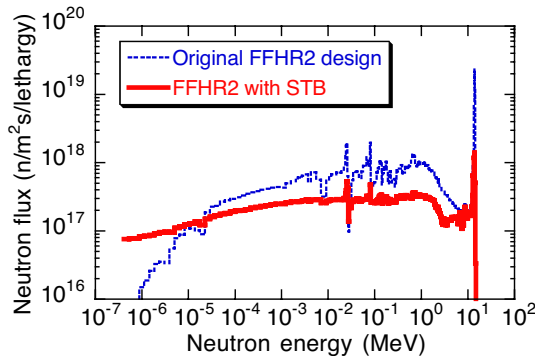FIG.3   Fast neutron flux at the first wall and the SC magnet.

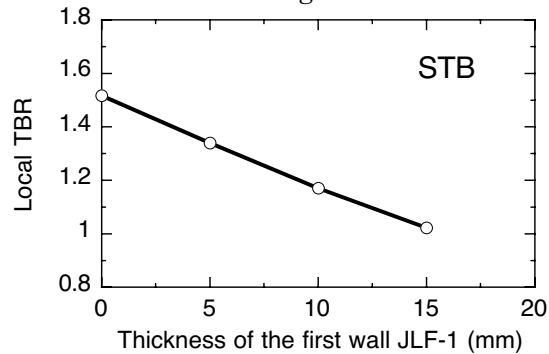FIG.4   Neutron energy spectra at the first wall with and without STB

FIG.5   Local TBR as a function of thickness of the first wall.

wall of JLF-1 (RAF) is reduced to $1.3 \times 10^{18}/m^2s$, which is about 140dpa in 30 years and 1/3 of the original flux $(4.2 \times 10^{18}/m^2s)$ as shown in Fig.3 and 4. At the same time the local TBR of about 1.2 is obtained as shown in Fig.2, where the TBR strongly depends on the thickness of the first wall as shown in Fig.5 due to absorption of decelerated neutrons. And furthermore, as shown in Fig.3, the fast neutron fluence to SC magnets is one order reduced to 5×10^{22} n/m^2, which is sufficient to keep $Tc/Tc_0 > 0.9$ for Nb_3Sn, for instance. Coil winding and SC materials choice issues are under investigation.

According to a finite element (FE) thermal analysis, the carbon armor surface temperature is about 1,600°C under conditions of nuclear heating with surface heat flux of $0.1MW/m^2$, effective thermal conductivity of 180W/m/K for C-Be_2C-C bonded armors of 16cm thickness and heat transfer coefficient of $6,000W/m^2/K$ for the bolted mechanical contact using a super-graphite sheet (100μm) [4] between the armor and the first wall of JLF-1. At the first wall the heat removal of about $1MW/m^2$ is required to self-cooling Flibe, where the packed-bed with Be pebbles (Fig.1) is promising to realize one order enhancement of heat transfer with a low flow rate [5] and to control REDOX chemical reactivity of molten salt [6]. Some key R&D issues are impurity shielding in edge plasma physics and armor tile lifetime. Carbon swelling and degradation of thermal and mechanical properties under high temperature neutron irradiation will determine the frequency of armor tile replacement, and a new replacement concept is proposed in Section 5. Fortunately the tritium inventory trapped in carbon and redeposited carbon is negligible at such high temperatures higher than 800°C[7], and the armor tiles are non γ-ray wastes.

3.   Modified Design Parameters of FFHR2

According to the requirements of neutron wall loading below $1.5MW/m^2$ and total blanket thickness of minimum 1.2m, the design parameters of FFHR2 are modified to those of FFHR2m, as shown in Table 1. The coil pitch parameter γ is 1.15 in FFHR2m1 to expand the blanket space and to reduce electromagnetic force, while γ is 1.25 in FFHR2m2 with inner shift of the plasma center as same as the standard condition in the present LHD [1]. FFHR2m2 is similar to the previous design LHR-S [8]. In both cases the major radius R is increased and the toroidal field B_0 is decreased, compared with FFHR2.

The self-ignition analyses have been performed with zero-dimensional particle and power balance equations and ignition access algorithm using PID control

TTABLE 1   Design parameters of   FFHR2m comparing with LHD and FFHR2.

Design parameters			LHD	FFHR2	FFHR2m1	FFHR2m2
Polarity	l		2	2	2	2
Field periods	m		10	10	10	10
Coil pitch parameter	γ		1.25	1.15	1.15	1.25
Coil major Radius	Rc	m	3.9	10	14.0	17.3
Coil minor radius	ac	m	0.98	2.3	3.22	4.33
Plasma major radius	Rp	m	3.75	10	14.0	16.0
Plasma radius	ap	m	0.61	1.2	1.73	2.80
Blanket space	Δ	m	0.12	0.7	1.2	1.1
Magnetic field	B0	T	4	10	6.18	4.43
Max. field on coils	Bmax	T	9.2	15	13.3	13.0
Coil current density	j	MA/m2	53	25	26.6	32.8
Weight of support		ton	400	2880	3020	3210
Magnetic energy		GJ	1.64	147	154	142
Fusion power	P_F	GW		1	1.9	3
Neutron wall load		MW/m2		1.5	1.5	1.3
External heating power	Pext	MW		70	80	100
α heating efficiency	ηα			0.7	0.9	0.9
Density lim.improvement				1	1.5	1.5
H factor of ISS95				2.40	1.92	1.76
Effective ion charge	Zeff			1.40	1.34	1.35
Electron density	ne(0)	10^19 m-3		27.4	26.7	19.0
Temperature	Ti(0)	keV		21	15.8	16.1
Plasma beta	<β>	%		1.6	3.0	4.1

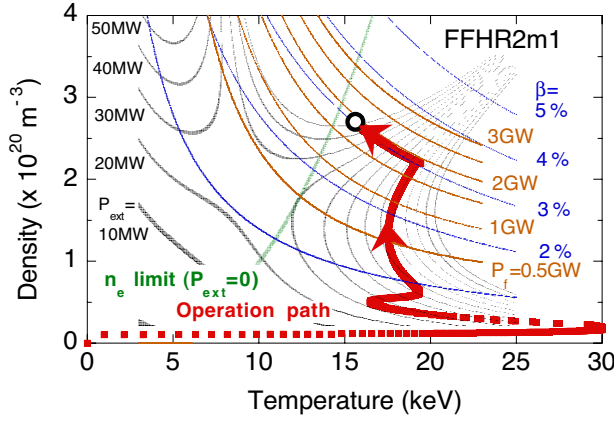[9], where the alpha confinement time ratio $\tau^*_\alpha/\tau_E = 3$ and parabolic density and temperature

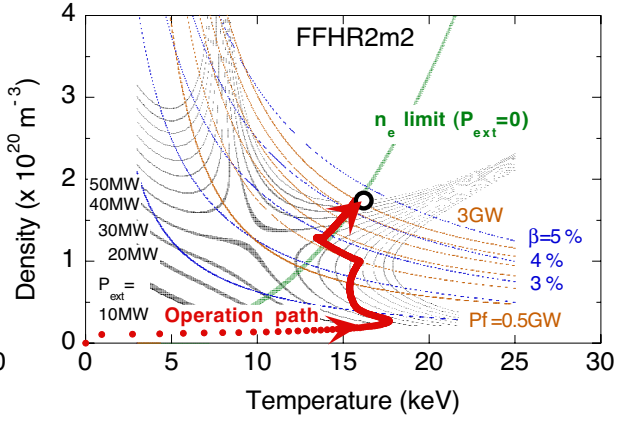Fig.6   POPCON plot for FFHR2ml showing the self-ignition operation path controlled under the density limit.

Fig.7   POPCON plot for FFHR2m2 showing the self-ignition operation path controlled under the density limit..

profiles are assumed. Figure 6 and 7 show the POPCON plots for FFHR2m1 and 2, respectively, where the fusion-power startup period is set at about 2 min and the self-ignition points are in the thermally stable region. In these analyses the density is controlled within 1.5 times the Sudo limit, as achieved in recent LHD results [10]. Therefore the enhancement factor H of the ISS95 confinement scaling is near the present LHD-achieved value of about 1.6. Evaluation studies using 3-dimensional equilibrium / 1-dimensional transport code [8] are also on going with neoclassical ripple transport as well as anomalous transport.

4.   Improved Design of the Coil-Supporting Structure

4.1.   Layout of Magnets

The layout of magnets is shown in Fig.8, where W and H are width and height of the helical coil in the cross-section. A high ratio of width to height is useful to reduce the maximum transverse field and to enlarge the blanket space, but it will bring problems for maintenance ports. The ratio of 2.0 was selected in this study as a moderate value. The pitch parameter γ of the helical coil is given by $(ma_c)/(lR_c)$, where R_c, a_c, l, and m are a coil major radius, a coil minor radius, a pole number, and a pitch number. It is set to 1.15 to reduce the electromagnetic force and to enlarge the distance between the helical coil and the plasma. The ratio of the highest magnetic field in the coil to the central toroidal field depends mainly on
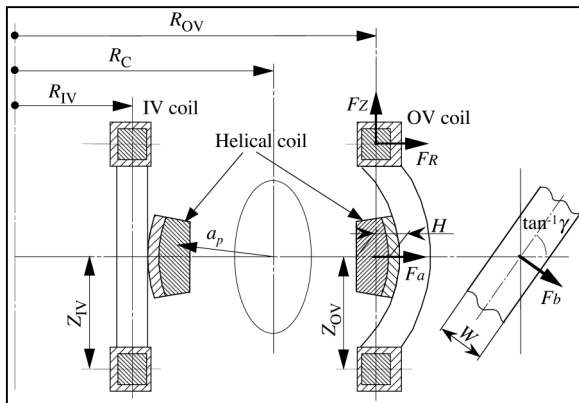

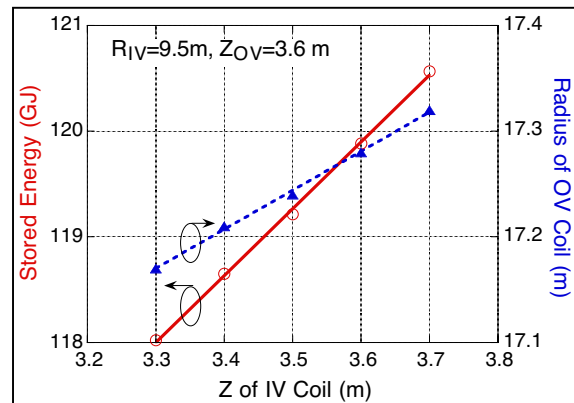Fig.8   Layout of helical coils, poloidal coils, and magnetic force.

Fig.9   Stored energy of FFHR2m1 with two pairs of poloidal coils.

the ratio H/a_c. The height was determined to make the highest field 13 T that is a conservative value for A15 superconductors, such as Nb_3Sn or Nb_3Al. As the results, the current density of the helical coil becomes 25 to 30 MA/m^2 that is a suitable value for the large coil including a mechanical support inside. Though high density of the coil current is useful to enlarge the space for blankets and for maintenance, it is restricted with cryogenic stability, mechanical strength and the highest field.

One set of poloidal coils is necessary to adjust the major radius of the plasma, the quadrupole field, and the stray field. In the case of two sets of poloidal coils, the number of degrees of freedom is six, which additionally makes it possible to reduce the field near the center of the torus and the total stored magnetic energy. The position of the coils is not determined uniquely because of the rest of the degrees of freedom. An adequate position was determined by considering the layout of the mechanical support. Figure 9 shows an example of the dependence of the stored energy on the height of IV coil. It is about 120 GJ that is 80% of that in the case of one pair of the poloidal coils.

4.2. Structural Analysis

Preliminary structural design for FFHR2m1 has been carried out. Electromagnetic forces on the coils are shown in Figures 10 and 11. Since sum of electromagnetic force on all coils is balanced, all coils were supported by each other. In considering the maintenance of blanket, large apertures are prepared at top, bottom and outer region. Since electromagnetic force on the helical coils is reduced by the 'force free' concept, the helical coils can withstand their electromagnetic forces by fixing them to inner and outer supporting structure around the mid-plane. A calculated stress by a FE model is shown in Fig. 12. Although the apparent maximum stress intensity exceeds 1,000 MPa here, it is due to insufficient accuracy in the present calculation. The maximum stress intensity is expected to be reduced less than 900 MPa by improving the accuracy. This value will be allowable for strengthened stainless steel.
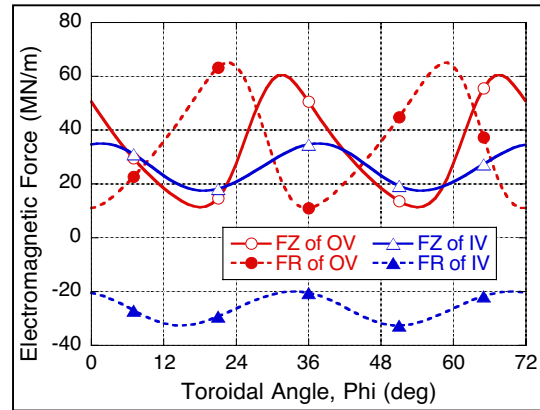

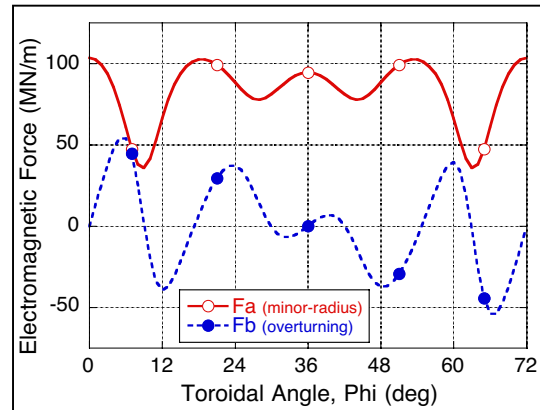Fig.10   *Electromagnetic forces on a helical coil of FFHR2m1.*

Fig.11   *Electromagnetic forces on poloidal coils of FFHR2m1.*

5.   Maintenance of In-Vessel Components

Figure 13 shows the typical poloidal cross sections in the 3D design of FFHR2m1 for a toroidal half pitch, where the field period m =10 and one pitch = 36°. Due to the simplified cylindrical supporting structure of helical and poloidal coils under the force reduced design, it is seen that large size maintenance ports can be opened at top, bottom, outer and inner sides of the torus, where the vacuum boundary is located just inside of the helical coils and supporting structure. Because the shielding zone of the blanket shown in Fig.1 is considered to be one of permanent structures, all blanket units can be supported on these shielding structures, which are helically wound and mainly supported at their bottom position.
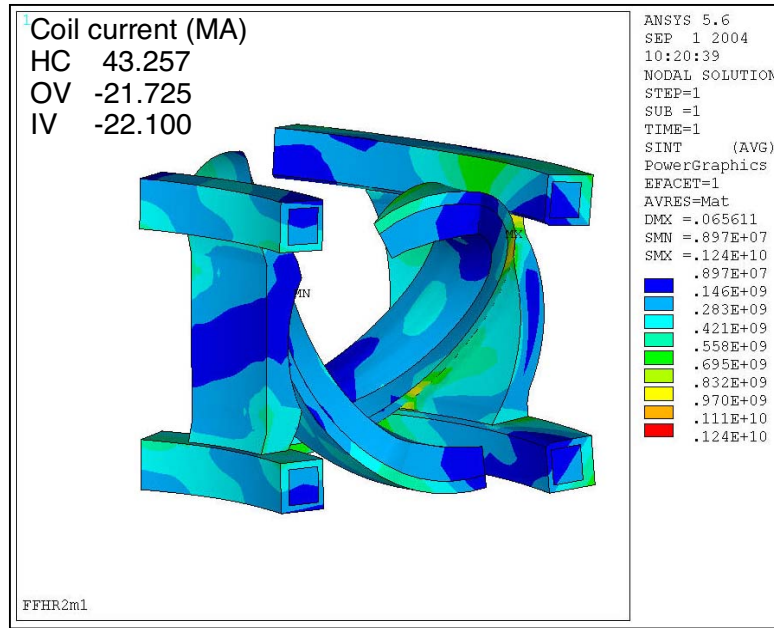
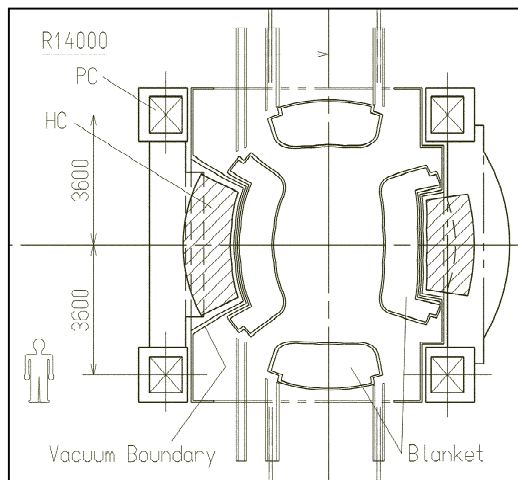*Fig.12   Finite element model of FFHR2m1.*

Fig.13a   The poloidal cross section at the toroidal angle θ=0° of FFHR2m1.

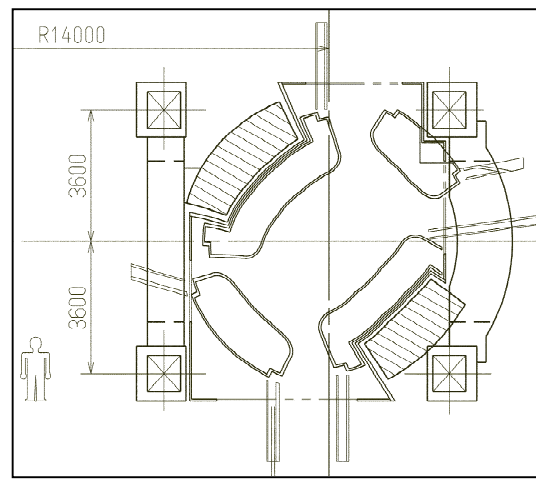*Fig.13b   The poloidal cross section at θ=36°/4 of FFHR2m1.*

Within the present databases, due to dimensional changes and degradation of thermal and mechanical properties of carbon under neutron irradiations, armor tiles of STB should be replaced during the planned inspection period. For this purpose, as shown in Fig.14, the "screw coaster" concept [11,12] is adopted using the merit of continuously winding helical structure, where the normal cross section of blanket is constant. Therefore the screw coaster can move along the helical guides at the edge of blankets with adjusting toroidal effects by flexible actuators. Then the coaster replaces the bolted tiles under remote handling.
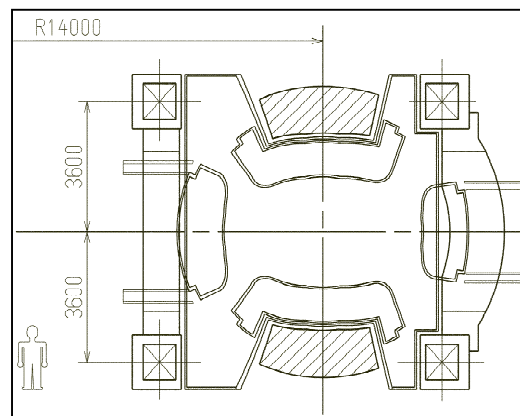

Fig.13c   The poloidal cross section at θ=36°/2 of FFHR2m1.
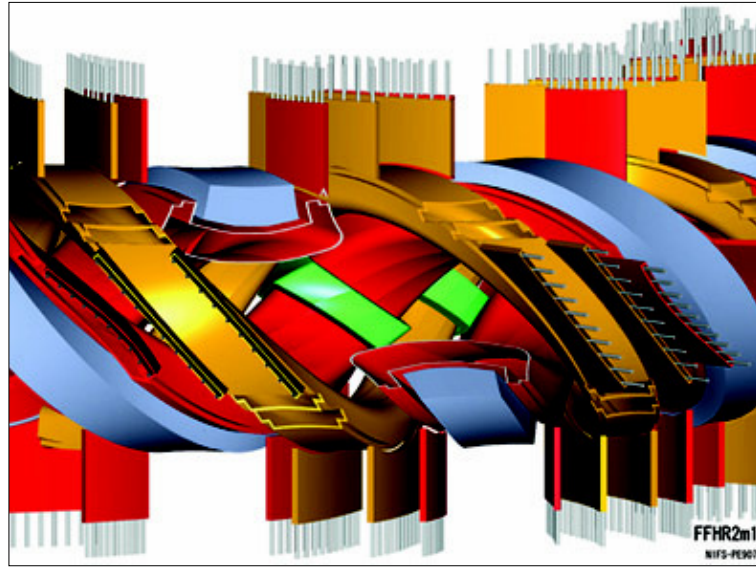
Fig.14   "Screw coasters" to replace STB armor tiles in FFHR2m1, where the helical coils and blankets with coolant pipes are only shown.
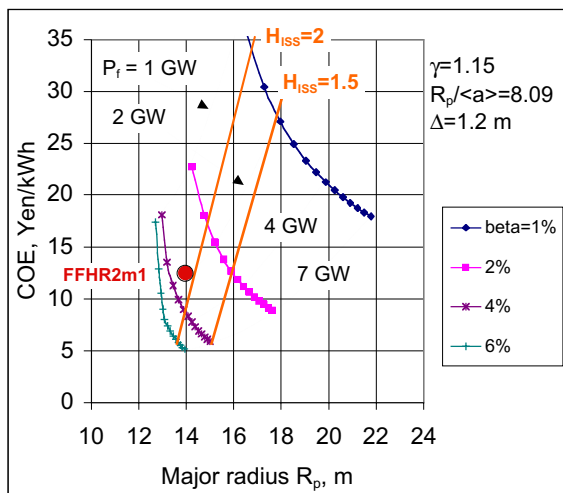

Fig.15   COE(Yen/kWh) of FFHR2m1, where the H factor of ISS95 is also indicated.
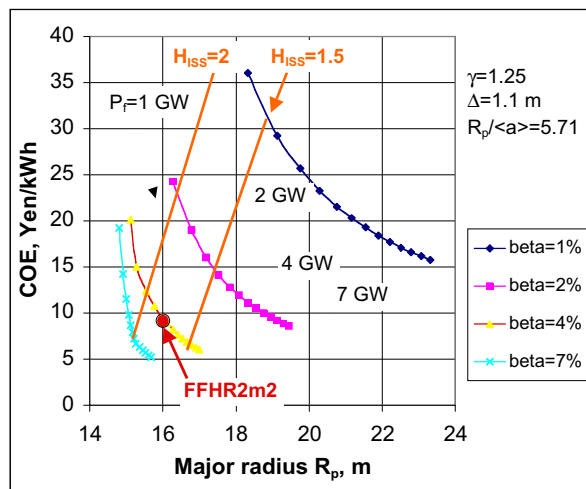

Fig.16   COE(Yen/kWh) of FFHR2m2, where the H factor of ISS95 is also indicated..

Detailed design of the divertor structure is under investigation, and it is seen in Fig.13 that there is an enough space for the double-null divertor pumping. As for replacement of divertor target tiles, the screw coaster can be basically used again during the planned inspection period.

6.   Cost Estimation

The Physics-Engineering-Cost (PEC) code has been developed in NIFS. Recently by modifying it to include blanket-shield design data, a new cost structure, new unit costs, and
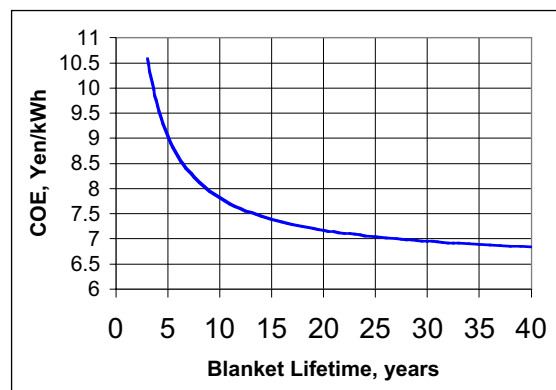

Fig.17   Variation of COE with blanket lifetime for FFHR2m2.

improved algorithms [13], the PEC code was calibrated by using it to model the ARIES-AT (advanced technology) tokamak and the ARIES-SPPS (stellarator power plant system), and it was found that the PEC Code COE estimates for each of these two cases differ from the published values by 5%, where those ARIES costs were escalated from 1992 $ to 2003 $ using an escalation factor of 1.223. Using this PEC code, COE's have been evaluated for FFHR2, FFHR2m1 and FFHR2m2, resulting in COE of 21.20, 12.95, and 9.53 Yen/kWh, respectively, as shown in Fig.15 and 16. The COE eventually decreases with increasing the reactor size, because the wall loading is fixed at about 1.5MW/m^2, and the fusion output increases, while the weight of coil supporting structure does not significantly increase as shown in Table1.

The effect of long-life blanket on COE is also evaluated by the PEC code with a model, which assumes an availability factor that varies from the usual maximum 0.85 as

$$f_{avail} = 0.85 - f_{avail} * 1.4\, G_w * t_m / Wt_b ,$$

where G_w = average neutron wall load (MW/m^2), 1.4 is the assumed peak to average ratio, t_m = blanket maintenance time (assumed to be 0.5 years), and Wt_b = blanket wall lifetime (MW-years/m^2). The result is shown in Fig.17. As the blanket lifetime increases from 5 to 30 years, the COE drops about 20% from 9 to 7 Yen/kWh. The savings result from a higher availability and from a lower cost for replacement blankets.

7. Conclusions

Design studies on the LHD-type heliotron D-T power reactor FFHR have focused on concept improvement by new design approaches to solve the key engineering issues of blanket space limitation and replacement difficulty. The main conclusions are:
  (1) The combination of improved support structure and long–life breeder blanket STB is quite successful.
  (2) The "screw coaster" concept is advantageous in heliotron reactors to replace in-vessel components.
  (3) The COE can be largely reduced by those improved designs.
  (4) The key R&D issues to develop the STB concept are elucidated.

References

[1] A. Komori et al., Plasma Phys. Contr. Fusion 45 (2003) 671.
[2] A. Sagara et al., 17th IAEA Fusion Energy Conf., Yokohama, FTP-3 (1998).
[3] R.W. Conn, G.L. Kulchinski et al., Nucl. Technology 26 (1975) 125.
[4] Y. Kubota et al., Fusion Eng. Des. 56-57 (2001) 205.
[5] S. Chiba et al., in these proceedings.
[6] S. Fukada et al., Proc. tritium 2004 (2004).
[7] A. Sagara et al., J. Nucl. Mater., 220-222 (1995) 627.
[8] K. Yamazaki et al., 18th IAEA Fusion Energy Conf., Sorrento, FTP2-12 (2000).
[9] O. Mitarai et al., Fusion Eng. Des. 70 (2004) 247.
[10] K. Nishimura et al., Annual Repo. of NIFS (2000) 13.
[11] A.Sagara, US-J Workshop on Fusion Power Reactors(P246), JAERI-memo 07-100(1995).
[12] A.Sagara et al, J. Nucl. Mater., 248 (1997) 147.
[13] T. J. Dolan et al., to be published in Fusion Science and Technology.